UC San Diego
UC San Diego Previously Published Works

Title

Artificial rheotaxis

Permalink

Journal

Science Advances, 1(4)

ISSN

Authors

Palacci, Jérémie

Sacanna, Stefano

Abramian, Anaïs

et al.

Publication Date

2015-05-01

DOI

Copyright Information

Peer reviewed

CONDENSED MATTER PHYSICS

Artificial rheotaxis

Jérémie Palacci,[1,2]* Stefano Sacanna,[3] Anaïs Abramian,[4] Jérémie Barral,[5] Kasey Hanson,[6] Alexander Y. Grosberg,[1] David J. Pine,[1] Paul M. Chaikin[1]

Motility is a basic feature of living microorganisms, and how it works is often determined by environmental cues. Recent efforts have focused on developing artificial systems that can mimic microorganisms, in particular their self-propulsion. We report on the design and characterization of synthetic self-propelled particles that migrate upstream, known as positive rheotaxis. This phenomenon results from a purely physical mechanism involving the interplay between the polarity of the particles and their alignment by a viscous torque. We show quantitative agreement between experimental data and a simple model of an overdamped Brownian pendulum. The model notably predicts the existence of a stagnation point in a diverging flow. We take advantage of this property to demonstrate that our active particles can sense and predictably organize in an imposed flow. Our colloidal system represents an important step toward the realization of biomimetic microsystems with the ability to sense and respond to environmental changes.

INTRODUCTION

In recent years, there has been a significant effort to design and synthesize active colloidal particles that mimic microorganisms. This has led to the development of self-propelled particles that can harvest a source of energy from their surroundings and convert it into directed motion (1–4). These systems share many properties with their biological counterparts: they exhibit a persistent random walk analogous to the run-and-tumble motility of bacteria, spermatozoa, or algae (5), and some synthetic realizations can even interact through chemical gradients and form "colonies," analogous to chemical-sensing organisms (6–9).

A key feature of motility is its interaction and response to its environment. The ability to sense its surroundings is crucial for living systems, and the migration up or down a gradient is called "taxis." Phototaxis of invertebrate larvae contributes to the vertical migration of marine plankton, which is thought to represent the biggest biomass transport on Earth (10). Chemotaxis, the migration in a chemical gradient, is used by sea urchin spermatozoa to guide themselves toward the egg (11) and by *Escherichia coli* bacteria to locate nutrient-rich environments (12). It is furthermore argued to be one of the key components in the formation of patterns and colonies of bacteria (13–15).

The presence of boundaries or obstacles can have a dramatic impact on the motion of motile microorganisms. Motile bacteria such as *E. coli* move in circles near surfaces (16, 17) and aggregate on substrates to form biofilms, which is at the root of many persistent bacterial infections (18). They reverse directions when spatially constricted and migrate preferentially through an array of V-shaped funnels (19). Additional effects emerge in a shear flow, for example, a flow past a no-slip solid surface, and numerous biological organisms exhibit rheotaxis or migration under shear. Rheotaxis of fish arises from a complex biological sensing (20, 21), but sperm (22, 23) and bacteria rheotaxis originate from physical mechanisms, such as a subtle interplay be-

tween velocity gradients and the helical shape of the flagella (24). *E. coli* bacteria as well as sperm cells exhibit direct and continuous upstream motility (positive rheotaxis) under shear flow (25, 26). Positive rheotaxis is also reported for *Pseudomonas aeruginosa* parasites as a coupling of the flow alignment with the twitching motility of the organism. This ability to go against the flow is argued to be beneficial for the ability to colonize environments, such as the bladder, that are inaccessible to other human pathogens (27). In these cases, the upstream migration is hypothesized to result from the coupled effect of the alignment of the body with the shear and the polar propulsion of the organism (25–29), resulting in migration toward the organs and areas where flows are flushing.

Here, we present a biomimetic colloidal system consisting of particles that exhibit a continuous positive rheotaxis under flow, near a solid substrate. Their upstream migration originates from a flow-induced alignment of the particles' polar heads. This restoring hydrodynamic torque competes with the thermal noise to align the particle, and the system is quantitatively described by an overdamped Brownian pendulum in an effective potential induced by the flow. We show that this mechanism allows for the development of adaptive particles that react to an environmental change. Synthetic rheotactic particles constitute a step toward the engineering of advanced microsystems with sensing, analogous to microorganisms.
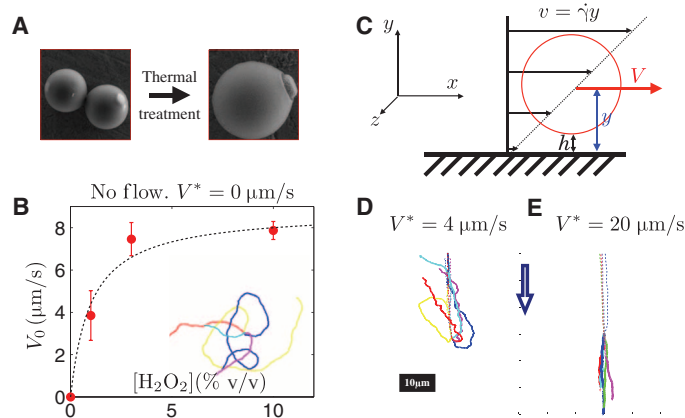
RESULTS

Our new particles are engineered starting from the colloidal surfers presented in Palacci *et al.* (7): composite particles featuring a hematite cube embedded in a polymeric sphere. We showed in a previous study that these particles become active under activation by a blue light in the presence of hydrogen peroxide fuel. They do not swim in bulk and only self-propel on a substrate in the considered experimental conditions (pH ~8.5). In a nutshell, the blue light triggers the photocatalytic decomposition of the hydrogen peroxide fuel by the hematite, creating chemical (O_2 and H_2O_2) gradients. Phoresis and osmosis are complementary interfacial phenomena (30). In a gradient, a free colloid migrates phoretically; alternatively, placed in the same gradient, a fixed surface will develop an osmotic flow in the opposite direction.

[1]Department of Physics, New York University, New York, NY 10003, USA. [2]Department of Physics, University of California, San Diego, La Jolla, CA 92093, USA. [3]Department of Chemistry, New York University, New York, NY 10003, USA. [4]Département de Physique, Ecole Normale Supérieure de Lyon, 69007 Lyon, France. [5]Center for Neural Science, New York University, New York, NY 10003, USA. [6]School of Materials Science and Engineering, College of Engineering, Georgia Institute of Technology, Atlanta, GA 30332, USA.
*Corresponding author. E-mail: palacci@ucsd.edu

Consequently, under activation of the hematite by light, the surface of the substrate develops an osmotic pumping flow, owing to the concentration gradient produced by the decomposition of the fuel (31, 32). The hematite part of the particle is pulled toward the substrate by the osmotic flow and the particle propels, surfing over the osmotic flow (7).

Using a thermal treatment (see Materials and Methods), we make the hematite inclusions to protrude out of the particle polymer matrix, obtaining the anisotropic particles shown in Fig. 1A. In a typical experiment, the particles are dispersed in a water-based solution containing hydrogen peroxide [varying concentrations of 1 to 10% (v/v)] and 5 mM tetramethylammonium hydroxide to adjust the pH to ~8.5. The suspensions are contained inside borosilicate square capillaries (Vitrotubes, 500 μm) that were previously cleaned by oxygen plasma. The capillaries are connected to a syringe pump (Harvard Apparatus 33) using standard microfluidic tubing (PEEK tubing, 125-μm inner diameter) and sealed using a ultraviolet curing glue (NOA 86, Nordland). A controlled and steady flux of solvent can be imposed in the capillary because of this setup. The experiments are observed through an inverted microscope (Nikon TE300) and recorded using a monochrome camera (EO-1312M) at a frame rate in the range 20 to 30 fps.

Fig. 1. Artificial rheotaxis of self-propelled particles. (**A**) Spherical 3-methacryloxypropyl trimethoxysilane polymer (TPM) containing a hematite cube (left) undergo a thermal treatment, resulting in an anisotropic particle with the hematite cube protruding out (right). (**B**) Dependence of the propulsion velocity V_0 on the concentration of hydrogen peroxide fuel (H_2O_2). The data are empirically fit (black dashed line) by the Michaelis-Menten kinetics, $V_0 = V_{max}[H_2O]/(B + [H_2O_2])$. Inset: Trajectories of different particles. We observe an isotropic propulsion in the absence of any flow and once activated by light. Note that the particles do not swim in bulk and only self-propel near a substrate. (**C**) Experimental setup. A syringe pump is connected to the capillary and induces a flow along the x direction. The particle (red sphere) resides at an altitude y near the bottom surface. It experiences a shear flow $v = \dot{\gamma} y$, where $\dot{\gamma}$ is the local shear rate, near the nonslip boundary condition. This results in a translational velocity of the particle $V(y/R)$, which depends on the ratio of the distance of the center of the particle to the wall with the radius R of the particle. (**D**) Trajectories of the particles for various flows and $V_0 \sim 8$ μm/s. The direction of the flow is indicated by the blue arrow. In the absence of any light, the particle is used as a flow tracer advected at velocity V^* (dashed line). Under light activation, the particle makes a U turn, and the hematite protrusion faces the flow (solid line). The alignment together with the polarity of the self-propulsion results in the upstream migration of the particles.

Under bright-field illumination, the particles are at equilibrium with the solvent and sit at a gravitational height (h_g) ~ 100 nm from the bottom wall (see Materials and Methods). The particles exhibit thermal translational and rotational Brownian motion, visible because of the optical contrast provided by the red hematite cube. When illuminated through the microscope objective (oil immersion, 100×; numerical aperture, 1.4) with blue light (Nikon Intensilight, equipped with a bandpass filter λ ~430 to 490 nm), the composite particles start to self-propel, with a distinct head and tail. The hematite cube leads the self-propelled particle, consistent with observations made using bare hematite particles as colloidal dockers for cargo transportation (33) and previous experiments with spherical composite particles directed by a magnetic field (7).

In the absence of an imposed flow, the particles exhibit isotropic self-propulsion with average velocity V_0 (Fig. 1B, inset, and movie S1), which varies with the concentration of hydrogen peroxide fuel and follows the Michaelis-Menten kinetics (Fig. 1B) (34, 35). The velocity linearly increases with hydrogen peroxide concentration at low concentrations and saturates at $V_0 \simeq 8$ μm/s for (H_2O_2) ≲ 5% (w/w).

The flux-driven flow is imposed in the x direction by a syringe pump connected to the capillary tube. This creates a steady Poiseuille flow so that the particles, confined near the nonslipping bottom surface, experience a shear flow. In the following, we denote V the velocity of the particle, and v is the velocity of the fluid at the particle's center. The velocity of the flow at the altitude y is $v(y) = \dot{\gamma} y$, where $\dot{\gamma}$ is the local shear rate (Fig. 1C).

In the case of a point particle advected by the flow, the two velocities are equal $V(y) = v(y)$. For the general case of a particle with finite radius R, the shear flow exerts a torque on the particle, which exhibits translational as well as rotational motion, and the ratio of the two velocities is a function of the dimensionless number y/R, where y is the distance of the center particle to the wall, $V(y)/v(y) = f(y/R)$. The function f is an increasing function of the ratio y/R and $f(y/R) \rightarrow 1$ far from the wall, $y \gg R$ (36).

Without activation by light, the particles are passive tracers of the flow. They translate while rolling, on average, at the altitude $y_g = R + h_g$ (Fig. 1C). The streamlines are straight lines along the x direction (Fig. 1, D and E, dashed line), and we characterize the flow measuring V_x. In the following, we use the notation * for the velocity of the particles measured in the absence of activation by the light, $V^* = V_x = f(y_g/R) \times v(y_g)$.

The dynamics of the particles in an external flow is drastically altered if the light is turned on and the self-propulsion is activated (Fig. 1, D and E, solid lines). The particles stop rolling and make a turn so that the hematite protrusion faces the imposed flow (Fig. 1D, solid line, and movies S2 and S3). For moderate flow, $V^* \leq V_0$, the particles migrate upstream once activated (movie S2). Increasing the flow velocity results in a better alignment of the particle displacement along the flow (movie S3). The angular probability distribution of the displacement $P(\theta)$ is flat for small flows, $V^* = 0.6$ μm/s, and narrows down as the flow velocity increases, leading to an acute distribution for $V^* = 20$ μm/s (Fig. 2C).

We do not observe any dependence of the phenomenon along the transverse position z in the channel. For fast flows, $V^* \geq 35$ μm/s, the particles detach from the wall due to the high shear. This regimen is not discussed in the paper.

In a set of independent experiments, we test the effect of the rotational motion of the particle on the translation velocity. The particle is
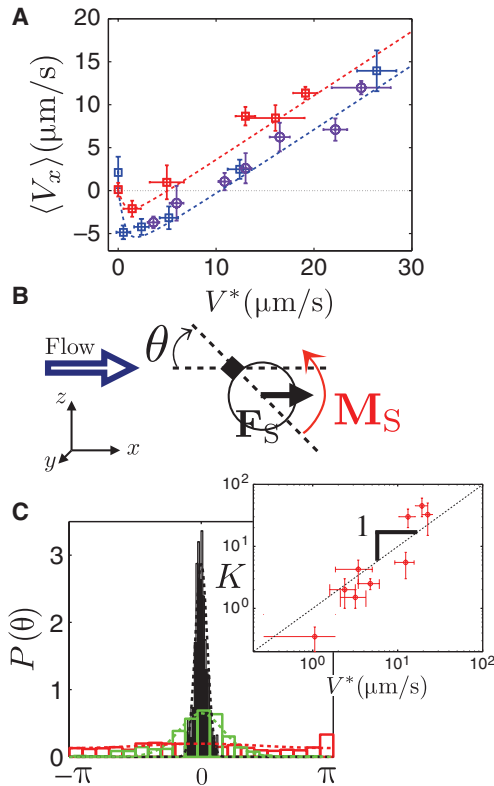
Fig 2. Mechanism in a nutshell and modelization. (**A**) Projection of the average velocity (V_x) along the direction of the flow as a function of V^*. The measurements are performed for various hydrogen peroxide concentration [H_2O_2 = 1, 3, and 10% (v/v)] (respectively red, blue, and purple symbols). The velocity V_0 depends on the fuel concentration. Fit of the experimental data with the model (see main text) for $V_0 = 4$ μm/s (red dashed line) and $V_0 = 8$ μm/s (blue dashed line) measured in the absence of any flow. (**B**) Model for the artificial rheotaxis and notation. We assume that the hematite component acts as a fixed pivot, linked to the substrate. We denote by θ the angle made by the tail-head direction of the particle with the flow (see sketch). The flow exerts a viscous drag F_s on the body of the particle, leading to a torque M_{Fs}, aligning the particle with the flow. The polarity of the particle induces an upstream migration. (**C**) Normalized angular distributions $P(θ)$ for increasing V^* in the range 0.6 to 20 μm/s. Expected Boltzmann distribution $P(θ) \propto \exp[K\cos(θ)]$ (dashed line) superimposed on the experimental histograms, with K as the fitting parameter. Inset: Measurements of K as a function V^* [log-log scale]. The data agree with the linear scaling $K = V^*/\tilde{v}_{exp}$ (black dashed line) predicted by our model. We obtain $1//\tilde{v}_{exp}$ = 1.5 ± 0.5 s/μm from the fit to the experimental data.

advected by the flow and, in the absence of any light, rotates. We can freeze the rotation of the particle using a uniform magnetic field to set the direction of the magnetic moment of the hematite. We do not observe any modification of V, whether the field it is applied transversely or along the flow. This result is consistent with (36) and shows that translation and rotation are decoupled at altitude y_g.

In the following, we use bracket notation ⟨⟩ for ensemble and time averages, where a typical ensemble includes 6 to 16 independent particles. We use the particle velocity ⟨V_x⟩ to quantify the experimental results. We measure ⟨V_x⟩ for various flows velocity V^* and for various self-propulsion velocities V_0, obtained by varying the concentration of hydrogen peroxide (Fig. 2A).

In the absence of flow, the propulsion is isotropic and the particles have equal probability to go against or along the flow, ⟨V_x⟩ = 0 μm/s. Negative values for ⟨V_x⟩ indicate positive rheotactic behavior of particles migrating upstream. For large flow velocities, ⟨V_x⟩ increases linearly with V^*.

DISCUSSION

Our understanding of the rheotaxis in this system has to do with how the active polar particle aligns with the flow. Under light activation, the hematite cube is pulled toward the surface owing to the induced osmotic flow at the wall (7, 33), the polymer body lags behind the center of the particle, and the viscous drag exerts a torque, ultimately resulting in the alignment of the particle by the flow. The polarity of the self-propelled particle induces the upstream migration. The osmotic pumping additionally pulls the particle closer to the wall, at the altitude $y_{on} = R + h_{on}$, where h_{on} is typically a few Debye length $λ_D$ ~4 nm. The greater proximity of the nonslipping wall slows down the particles: $V(y_{on}) = f(y_{on}/R) \times v(y_{on})$ with $f(y_{on}/R) < f(y_g/R)$. We express $V(y_{on})$, the advected velocity, in terms of the measurement V^*:

$$V(\dot{y}_{on}) \sim \frac{f(y_{on}/R)}{f(y_g/R)} V^*. \qquad (1)$$

We now present a quantitative description based on this simple model. We use the bold notation for vectors and denote by η the viscosity of the solution, equal to the viscosity of water to a very good approximation. We assume, for the sake of simplicity, that, under light activation, the hematite cube is a "fixed" pivot, and we use the notation presented in Fig. 2B.

The flow exerts on the particle a Stokes drag $\mathbf{F}_S = 6\pi\eta R\mathbf{v}$ leading to a torque $\mathbf{M}_S = 6\pi\eta R^2 v\sin\theta \mathbf{e}_z = M_S\mathbf{e}_z$, which tends to align "downstream" from the hematite pivot (Fig. 2B). There is a competition between the restoring torque and the thermal rotational diffusion of the particle around the hematite pivoting point. Provided the low Reynolds dynamics of the particles in the experiment, $Re \sim 10^{-5}$, the problem is formally equivalent to an overdamped Brownian pendulum in a "gravitational" field, the gravity here being replaced by an effective potential (37)

$$U_{eff}(\theta) = -6\pi\eta R^2 v\cos\theta. \qquad (2)$$

Using this analogy, the equation followed by the angular probability distribution $P(\theta, t)$ is given by the Smoluchowski equation (37): $\partial_t P(\theta, t) = D_\theta \partial_\theta [\partial_\theta P(\theta, t) + \beta M_S P(\theta, t)]$, where D_θ is the rotational diffusion coefficient of the particle, ∂_θ is the angular component of the gradient, and $\beta = 1/k_B T$.

The steady-state solution is given by the pseudo-Boltzmann distribution $P(\theta) \propto \exp(-\beta U_{eff})$. After normalization, and using the expression of the effective potential U_{eff} (Eq. 2), we obtain:

$$P(\theta) = \frac{1}{I_0(K)} e^{K\cos\theta}, \qquad (3)$$

where I_0 is the modified Bessel function of the first kind of 0th order (38) and $K = 6\pi\eta\beta R^2 v = v/\tilde{v}$. In our present experimental conditions, we estimate from the former equation, $\tilde{v} \sim 0.2$ μm/s.
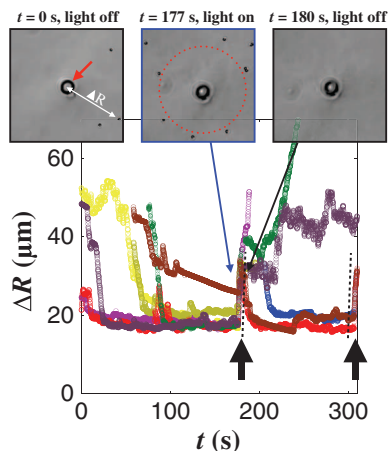
Fig. 3. Self-organization in a nonuniform flow field. A pulled micropipette is placed above a glass substrate where artificial swimmers reside, dispersed in a fuel solution. The same fuel solution is ejected out of the nozzle of the micropipette (red arrow) inducing a diverging flow decaying from the tip. Initially, the particles are randomly distributed in the sample. Under light activation, the particles migrate toward the tip and stop at a finite distance. They form a circle around the tip. Turning off the light, the particles are flushed away by the flow. The behavior is quantified the distance $\Delta R(t)$, as a distance to the nozzle (one color for each particle). The particles move toward the tip and stay at a finite and constant distance (inset, $t = 177$ s). Turning off the light (black arrows), they are flushed away by the flow (inset, $t = 180$ s). The velocity with which the particles are ejected provides a measure of the flow velocity at the position of mechanical equilibrium. We measure $U^* = 7 \pm 1$ µm/s (black dashed line), in agreement with our expectations for the considered active particles. Turning on the light, the particles migrate against the flow and reform a circle at the same distance from the tip.

We compare the theoretical expectations for the orientation distribution function of particle (Eq. 3) with the experiment. We measure experimentally the angular distribution of the displacement as the angle made by the displacement of the particles, with respect to the direction x of the flow, over a time interval of $\Delta t = 0.2$ s, much shorter than the typical persistence time of self-propulsion ~8 s, determined from the trajectories. Given the polarity of the moving composite particle, this measurement reflects the orientation of the particle, while being much more experimentally robust and accurate than the determination of the orientation vector of the particle. The distributions are obtained for 100 to 600 angles per particle for ~10 independent particles. The results show good agreement between the pseudo-Boltzmann distribution and the experimental measurements (Fig. 2C). We use the distributions to extract the dependence of the width K as a function of the particle velocity V^*. The data agree, over two decades, with the linear scaling predicted by our model, $K = V^*/\tilde{v}_{exp}$ with $1/\tilde{v}_{exp} = 1.5 \pm 0.5$ s/µm (Fig. 2C, inset). One should note that the model assumes that the hematite cube provides a rigid fixed pivot, whereas we observe in the experiment that it is sliding on the substrate. As a consequence, we expect to overestimate the strength of the restoring torque from the model, in line with the observed result.

Given the angular distribution $P(\theta)$, one can derive the expression for the average velocity $\langle V_x \rangle$. In our simple model, the instantaneous velocity of the particle in the reference frame of the laboratory is given

by $V_x = V(y_{on}) - \cos\theta V_0$, where $V(y_{on})$ is the particle velocity at the altitude y_{on} and $-\cos\theta V_0$ is the contribution of the self-propulsion due to the alignment of the particle by the flow. Using Eq. 1, we average over both time and an ensemble of independent particles and obtain:

$$\langle V_x \rangle = \left\langle \frac{f(y_{on}/R)}{f(y_g/R)} V^* - V_0 \cos \theta \right\rangle = \frac{f(y_{on}/R)}{f(y_g/R)} V^* - V_0\langle\cos\theta\rangle$$
$$= \alpha V^* - \frac{I_1(K)}{I_0(K)} V_0, \tag{4}$$

where $I_1 = \int P(\theta)\cos\theta d\theta$ is the modified Bessel function of the first kind of 1st order (38) and $\alpha = \dfrac{f(y_{on}/R)}{f(y_g/R)}$ is smaller than 1.

We compare this simple model with the experimental measurements gathered in Fig. 2A using the value for $\tilde{v}$ extracted from the experiment (Fig. 2D) and the velocity of self-propulsion, V_0, measured in the absence of flow (Fig. 1B). We obtain an excellent quantitative agreement between the model provided by Eq. 4 (dashed lines) and the experiment (data points) as visible in Fig. 2, using $\alpha \sim 0.75$ for all the sets of self-propulsion and hydrogen peroxide concentration [1, 3, and 10% (v/v)]. This value for α corresponds to a change of height from $h_s \sim 100$ nm to $h_s \sim 10$ nm according to Goldmann *et al.* (36) and is in good agreement with our estimates for the change of altitude of the particles, under activation of the particles by the light and change from the equilibrium sedimentation height to a few Debye length.

A similar mechanism has been discussed for mammalian sperm cells and compared to a dynamical model using resistive force theory. Sperm cells spontaneously swim toward surfaces, heads on. The tails therefore explore, on average, regions of higher flow velocity than the head, resulting in a net torque and shear-induced rectification (26).

The observed phenomenon exhibits an interesting feature: the existence of a stable stagnation position for the particles in a diverging flow field (Fig. 2A). We harness this property to design a system of adaptive active particles that self-organize in a nonuniform shear flow. We obtain a diverging flow by placing the tip of a pulled micropipette a few microns above a glass substrate, immersed in a solution of rheotactic particles and hydrogen peroxide (Fig. 3, insets). The flow velocity and the shear are decaying from the nozzle. In the absence of activation by light, the flow flushes the particles away from the pipette. Once activated by the light, the particles spontaneously gather along a circle around the tip, at a finite distance ΔR_0 from the tip and determined by the stagnation velocity $\langle V_x \rangle = 0$ for nonzero U^* (Fig. 3, insets, and movie S4). Turning off the light, the particles are immediately flushed away from the tip with a velocity of 7 µm/s, in agreement with the model (Fig. 3). They reorganize and reform the circle at the same distance ΔR_0 once the light is reactivated, with the flow being unchanged. This is a step toward the achievement of an adaptive artificial system that organizes in an external flow.

In this paper, we engineered synthetic microparticles that can sense their environment and spontaneously migrate against an imposed external flow near a surface, thus exhibiting a rheotactic behavior. This effect originates in the alignment of the body of a polar self-propelled particle by a drag anisotropy. It can result from a shape anisotropy (39) or the attraction of one part of the body to a solid substrate (rheotaxis on a surface), as for mammalian sperm cells (26) or our particles. Our system is formally identical to an overdamped Brownian pendulum in an effective nonequilibrium potential, induced by the flow, and is quantitatively described by a Smoluchowski equation for the angular

distribution. This system shows a step forward in the synthesis of artificial microsystems with advanced biomimetic functionalities because analogous strategies are used by many microorganisms to colonize regions against the flow (25, 27–29).

MATERIALS AND METHODS

Colloidal synthesis and heat treatment

The photocatalytic hematite cubes were prepared following the method described by Sugimoto et al. (40). Briefly, a sodium hydroxide solution (21.6 g of NaOH in 100 ml of Millipore water) was dripped in an iron chloride solution (54 g of FeCl$_3$·6H$_2$O in 100 ml of Millipore water), and the resulting gel was left undisturbed at 100°C in a closed Pyrex bottle for 8 days. The resulting hematite cubes were first washed by centrifugation and dispersed in deionized water and then encapsulated into polymerizable silicon oil droplets as follows.

First, TPM was hydrolyzed to water-soluble silanols by vigorously mixing 5 ml of TPM and 100 ml of Millipore water until all the TPM was dissolved and a clear solution was formed (usually 5 to 7 hours). Then 0.75 ml of ammonia [NH$_3$, 37 weight percent (wt %)] was added to a 30-ml aqueous dispersion of hematite cubes (final concentration, 10 wt %) containing a total of 15 ml of hydrolyzed TPM, while kept under vigorous magnetic stirring. The addition of ammonia causes a polycondensation reaction between metastable water-soluble silanols to produce insoluble silsesquioxanes that phase-separate nucleating monodisperse droplets as further described in (41). Each hematite cube, initially suspended in the water phase, acts as a nucleation site for the formation of an oil droplet, thus producing polymer droplets with a single inorganic inclusion. The reaction was sampled every 15 min, and the particle growth was monitored with optical microscopy. To increase the size of the TPM droplets, the reaction was fed with more hydrolyzed TPM until the particles reached the desired size. The particles were then polymerized by adding 0.5 mg of 2,2′-azobisisobutyronitrile (AIBN) to the dispersion preheated at 80°C and kept at this temperature for 3 hours. The polymerized particles were then dried in air at 80°C to a solid powder and finally further heated at 700°C for 5 hours. During this heat treatment, the organic material contained in the TPM matrix burns, causing a severe particle shrinkage and the consequent protrusion of the hematite cubes.

Sedimentation height

The sedimentation height, $h_g = \dfrac{kT}{mg}$, is defined as the height for which the gravitational energy of the particle balances the thermal energy in the system. For a typical particle, the typical radius of the TPM (density 2.0) sphere is $R \sim 1$ µm, and the hematite cube (density 5.25) of size 600 nm gives a sedimentation height for the composite particle, $h_g \sim 100$ nm.

SUPPLEMENTARY MATERIALS

Movie S1. Dynamics of the self-propelled particles in the absence of any external flow and shear.
Movie S2. Dynamics of the self-propelled particles under shear, at slow flow ($V^* = 4$ µm/s) and for a self-propulsion velocity of the particles ($V_0 = 8$ µm/s).
Movie S3. Dynamics of the self-propelled particles under shear, at fast flow ($V^* = 20$ µm/s) and the self-propulsion velocity of the particles ($V_0 = 8$ µm/s).
Movie S4. Organization of the particles in a diverging flow.

REFERENCES AND NOTES

1. W. Wang, W. Duan, S. Ahmed, T. E. Mallouk, A. Sen, Small power: Autonomous nano- and micromotors propelled by self-generated gradients. Nano Today 8, 531–554 (2013).
2. S. Sengupta, M. E. Ibele, A. Sen, Fantastic voyage: Designing self-powered nanorobots. Angew. Chem. Int. Ed. Engl. 51, 8434–8445 (2012).
3. J. Wang, W. Gao, Nano/microscale motors: Biomedical opportunities and challenges. ACS Nano 6, 5745–5751 (2012).
4. I. Buttinoni, G. Volpe, F. Kümmel, G. Volpe, C. Bechinger, Active Brownian motion tunable by light. J. Phys. Condens. Matter 24, 284129 (2012).
5. M. E. Cates, J. Tailleur, When are active Brownian particles and run-and-tumble particles equivalent? Consequences for motility-induced phase separation. Europhys. Lett. 101, 20010 (2013).
6. I. Theurkauff, C. Cottin-Bizonne, J. Palacci, C. Ybert, L. Bocquet, Dynamic clustering in active colloidal suspensions with chemical signaling. Phys. Rev. Lett. 108, 268303 (2012).
7. J. Palacci, S. Sacanna, A. Preska Steinberg, D. J. Pine, P. M. Chaikin, Living crystals of light-activated colloidal surfers. Science 339, 936–940 (2013).
8. E. F. Keller, L. A. Segel, Model for chemotaxis. J. Theor. Biol. 30, 225–234 (1971).
9. H. Masoud, M. J. Shelley, Collective surfing of chemically active particles. Phys. Rev. Lett. 112, 128304 (2014).
10. G. Jékely, J. Colombelli, H. Hausen, H. Hausen, K. Guy, E. Stelzer, F. Nédélec, D. Arendt, Mechanism of phototaxis in marine zooplankton. Nature 456, 395–399 (2008).
11. B. M. Friedrich, F. Jülicher, Chemotaxis of sperm cells. Proc. Natl. Acad. Sci. U.S.A. 104, 13256–13261 (2007).
12. H. C. Berg, Motile behavior of bacteria. Physics Today 53, 24–29 (2000).
13. E. O. Budrene, H. C. Berg, Dynamics of formation of symmetrical patterns by chemotactic bacteria. Nature 376, 49–53 (1995).
14. E. O. Budrene, H. C. Berg, Complex patterns formed by motile cells of Escherichia coli. Nature 349, 630–633 (1991).
15. M. E. Cates, D. Marenduzzo, I. Pagonabarraga, J. Tailleur, Arrested phase separation in reproducing bacteria creates a generic route to pattern formation. Proc. Natl. Acad. Sci. U.S.A. 107, 11715–11720 (2010).
16. A. P. Berke, L. Turner, H. C. Berg, E. Lauga, Hydrodynamic attraction of swimming microorganisms by surfaces. Phys. Rev. Lett. 101, 038102 (2008).
17. R. Di Leonardo, D. Dell'Arciprete, L. Angelani, V. Lebbaand, Swimming with an image. Phys. Rev. Lett. 106, 038101 (2011).
18. J. W. Costerton, P. S. Stewart, E. P. Greenbergand, Bacterial biofilms: A common cause of persistent infections. Science 284, 1318–1322 (1999).
19. P. Galajda, J. Keymer, P. Chaikin, R. Austin, A wall of funnels concentrates swimming bacteria. J. Bacteriol. 189, 8704–8707 (2007).
20. G. P. Arnold, Rheotropism in fishes. Biol. Rev. Camb. Philos. Soc. 49, 515–576 (1974).
21. J. C. Montgomery, C. F. Baker, A. G. Carton, The lateral line can mediate rheotaxis in fish. Nature, 389, 960–963 (1997).
22. F. P. Bretherton, L. Rothschild, Rheotaxis of spermatozoa. Proc. R. Soc. B 153, 490–502 (1961).
23. T. J. Pedley, J. O. Kessler, Hydrodynamic phenomena in suspensions of swimming microorganisms. Annu. Rev. Fluid Mech. 24, 313–358 (1992).
24. Marcos, H. C. Fu, T. R. Powers, R. Stocker, Bacterial rheotaxis, Proc. Natl. Acad. Sci. U.S.A. 109, 4780–4785 (2012).
25. T. Kaya, H. Koser, Direct upstream motility in Escherichia coli. Biophys. J. 102, 1514–1523 (2012).
26. V. Kantsler, J. Dunkel, M. Blayney, R. E. Goldstein, Rheotaxis facilitates upstream navigation of mammalian sperm cells. ELife 3, e02403 (2014).
27. Y. Shen, A. Siryaporn, S. Lecuyer, Z. Gitai, H. A. Stonend, Flow directs surface-attached bacteria to twitch upstream. Biophys. J. 103, 146–151 (2012).
28. J. Hill, O. Kalkanci, J. McMurry, H. Koserand Hydrodynamic surface interactions enable Escherichia coli to seek efficient routes to swim upstream. Phys. Rev. Lett. 98, 068101 (2007).
29. Y. Meng, Y. Li, C. D. Galvani, G. Hao, J. N. Turner, T. J. Burr, H. C. Hochand, Upstream migration of Xylella fastidiosa via pilus-driven twitching motility. J. Bacteriol. 187, 5560–5567 (2005).
30. J. L. Anderson, Colloid transport by interfacial forces. Annu. Rev. Fluid Mech. 21, 61–99 (1989).
31. U. M. Cordova-Figueroa, J. F. Brady, Osmotic propulsion: The osmotic motor. Phys. Rev. Lett. 100, 158303 (2008).

32. R. Golestanian, T. B. Liverpool, A. Ajdari, Propulsion of a molecular machine by asymmetric distribution of reaction products. *Phys. Rev. Lett.* **94**, 220801 (2005).

33. J. Palacci, S. Sacanna, A. Vatchinsky, P. M. Chaikin, D. J. Pine, Photoactivated colloidal dockers for cargo transportation. *J. Am. Chem. Soc.* **135**, 15978–15981 (2013).

34. L. Michaelis, M. L. Menten, The kinetics of the inversion effect. *Biochemische Zeitschrift* **49**, 333–369 (1913).

35. J. R. Howse, R. A. L. Jones, A. J. Ryan, T. Gough, R. Vafabakhsh, R. Golestanian, Self-motile colloidal particles: From directed propulsion to random walk. *Phys. Rev. Lett.* **99**, 048102 (2007).

36. A. J. Goldman, R. G. Cox, H. Brenner, Slow viscous motion of a sphere parallel to a plane wall: II. Couette flow. *Chem. Eng. Sci.* **22**, 653–660 (1967).

37. J.-L. Barrat, J.-P. Hansen, *Basic Concepts for Simple and Complex Liquids* (Cambridge Univ. Press, Cambridge, ed. 1, 2003).

38. S. Wolfram, *The Mathematica® Book, Version 4* (Cambridge Univ. Press, Cambridge, 1999).

39. B. ten Hagen, F. Kümmel, R. Wittkowski, D. Takagi, H. Löwen, C. Bechinger, Gravitaxis of asymmetric self-propelled colloidal particles. *Nat. Commun.* **5**, 4829 (2014).

40. T. Sugimoto, K. Sakata, A. Muramatsu, Formation mechanism of monodisperse pseudocubic α-Fe_2O_3 particles from condensed ferric hydroxide gel. *J. Colloid Interface Sci.* **159**, 372–382 (1993).

41. L. Rossi, S. Sacanna, W. T. M. Irvine, P. M. Chaikin, D. J. Pine, A. P. Philipse, Cubic crystals from cubic colloids. *Soft Matter* **7**, 4139–4142 (2011).

Citation: J. Palacci, S. Sacanna, A. Abramian, J. Barral, K. Hanson, A. Y. Grosberg, D. J. Pine, P. M. Chaikin, Artificial rheotaxis. *Sci. Adv.* **1**, e1400214 (2015).